OPTIMIZATION DESIGN ON PLATE-RIB STRUCTURE FOR CERTAIN KINDS OF AIRCRAFT

Y. C. Deng, C. Sun
Shen Yang Aircraft Design and Research Institute, AVIC1, P.R.C.

Keywords: *Plate-Stiffener Structure of Aircraft, Topology Optimization, Size Optimization, FEM & FSD, Experiment Demonstration*

Abstract

Plate-rib structures have a wide application on modern aircraft, no matter they are bulk heads in fuselage, or spars/strength ribs in wing and empennage, all of them are typical plate-rib components. In order to deal with the optimal design of plate-rib structure, first of all, the topology optimization based on 'gradient threshold' is utilized, so that the main load paths can be obtained; and then, rod and plate elements are used to simulate the component and the corresponding FE model are constructed; finally, the design variables are considered to be sizing which are plate's thickness and rib's section-area, and the fully stressed design(FSD) criterion are adopted as optimization strategy to obtain the optimal solution. Numerical results of several examples express that on the condition of the equal structural stiffness, the proposed method can reduce the structural weight from 5% to 20% comparing with the traditional approach based on engineering experience. Static test in the qualified laboratory has been done the first time in our country. Stiffness experiment results demonstrated that on the condition of the equal structural weight, the proposed approach can improve the structural stiffness from 10% to 30% comparing with the traditional one. Study in detail, we can find that comparing among the plate-rib structure(ribs are layout in the load paths) and the truss-like structure(rods are layout in the load paths) as well as conventional plate-rib structure(not all ribs are layout in the load paths), each has its own characteristic, respectively. The former is lightest in weight, the middle is lowest in stress and the latter is highest in stress. Therefore, according to the

characteristic of the components, the designer can select different kinds of structural layout for purpose. Usually, aircraft belongs to thin-walled airframe; its characteristic of stiffness is the key point, especially for modern air vehicle. It means that the proposed design approach for plate-rib structure is suitable to the light-weight design for bulk heads of fuselage, short spars and ribs of wing and empennage.

1 General Introduction

It is now well-known that the most important work on aircraft conceptual design is to determine the total weight, configuration and size as well as cost [1], no matter for military aircraft or civil airplane. Weight is not only concerned with performance, but with aircraft cost as well. If the aircraft performance does not meet the mission requirement, especially for fighter, then the consumer will refuse it. However if the price of the plane is too high, especially for civil airliner, then the market will not accept it. Therefore, on the basis of satisfying the design purpose, the aircraft weight saving is not only the pursuit of all aircraft designers, but also a motif of aircraft design.

With today's advances in science and technology, that is to say, we suppose that with our engine's capability, avionics and payload unchanged, the only effective way to reduce weight is through a lighter airframe.

Accompanied with the mature of structure optimization, especially for the development of computer soft and hard ware as well as experiment technique, which provide the possibility and operation for innovative design of aircraft structure [2]. For instance, American ALTAIR engineering limited company was the

first to utilize structural topology optimization to design and manufacture the leading edge rib of A380, as shown in figure 1 and 2, respectively [3]. Also some researchers applied this method on structure layout of aircraft control surfaces [4], and thin-walled structures, such as bulk heads [5, 6] and beams [7] etc.
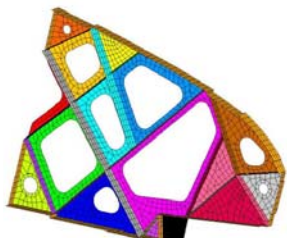
Fig. 1. Rib of designed   Fig. 2. Rib of fabricated

Looking ahead to the future, in terms of redesigning aircraft, whether it is conventional or unconventional configuration, we know that bulk heads are prime areas to be considered for weight savings. The bulk heads which bear most of loads usually can be outlined typically several variety of plate-rib/stiffener structure. In present studies, three steps are set forth, including (1) confirm the load paths of component by topology optimization based on 'gradient threshold' concept[2~4] which was proposed by the author previously, and set the ribs/stiffeners on the place of load paths; (2) bar and membrane elements are used to simulate the component and the corresponding FE model are built; (3) the design variables are considered to be sizing variables which are plate's thickness and stiffener's section-area, side constraints are also concluded, meanwhile, the fully stressed design (FSD) criterion are adopted as optimization strategy.

2 Basic Approaches

There are three ways to solve practical engineering optimal problem. First is dependent on the accumulation of designers with experience and intuitive judgment. Next is through test to select the better one by way of comparison. Last is to establish the mathematical model so that optimal solution can be found.

With regard to the plate-rib structures of aircraft, no matter fuselage frames or wing spars and ribs, their best structure layout is the most

concerned by designer and generally, this obstacle is solved by designer's background experience and intuitive judgment, which is the first way above mentioned.

In this paper, the approach is to adopt the integration strategy to deal with the plate-rib structural problem. First, the optimal layout of structural material is given, i.e. given the main load paths of the components through structural topology optimization. Next, FE analysis model and FSD optimization model are constructed respectively, and then, the optimal design can be acquired by numerical iterations. Wherever, the output of the former is the input of the latter. Finally, experiment demonstration has been done through several occasions of static bending and shear load test in a qualified lab.

2.1 Optimal Layout of Structural Material

Plate-rib/stiffener structure of aircraft is typical of a thin-walled component, so it is an advantage to increase its inboard's stiffness. From the above characteristic, we can propose such a computational model: under the condition of certain amount of material, find the best direction and arrangement of stiffeners with maximum structural stiffness (one kind of energy metric). The determined ribs/stiffeners are the efficient layout of material, i.e. are structural load paths. The general formulation of this model can be mathematically expressed as follows:

$$Minimize \qquad C\left(\vec{X}\right) = \vec{F}^T \cdot \vec{U}\left(\vec{X}\right)$$

$$Subject \quad to \quad \begin{cases} s\left(\vec{X}\right)\Big/ S_0 \leq f \\ 0 < x_i \leq 1 \qquad i = 1, \cdots, N \end{cases}$$

This model utilizes the typical topology optimization objective and constraint, which is to minimize global compliance subject to a volume fraction constraint. Where $\vec{X}$ is the vector of design variable, here which is pseudo-density; $c(\vec{x})$ is the scalar of global structure compliance measure-of-merit; $\vec{F}$ is the vector of node-force; $\vec{U}(\vec{x})$ is the vector of node-displacement; $s(\vec{X})$ is the effective area of plate-rib component during design iterations; S_0 is the total area of plate-rib component; f is

percentage of material used and N is the number of design variables.

To solve the above, the author set forth the concept of 'gradient threshold' and 'constraint compensation' to formulate an algorithm for determining the rational layout of structural material.

The definition of gradient threshold is that partial-derivative of compliance to pseudo-density is calculated first, then this gradient vector is standardized and finally the middle value of the standardized vector is selected and regarded as the threshold. During the iterations of optimization, if the pseudo-density's value is greater than the threshold's value, then it is exceeded, but not bigger than one (upper bound); if the pseudo-density's value is smaller than the threshold's value, then it is decreased, but not smaller than 0.01 (lower bound). The constraint compensation is defined as the change of constraint due to the exceed value of design variables equals to the change of constraint due to the deduction value of design variables. This strategy can ensure the pseudo-densities to be in the range between lower and upper bounds of design variables.

Imposing the strategy of gradient threshold and constraint compensation on topology optimization of aircraft wing box, the author obtained some useful results [4] from it. Something is found for more study in detail to the algorithm in reference 4: (1) when the amount of material is between 40%~60%, no matter the optimal graph or optimal values of pseudo-density are all perfect; (2) when the amount of material is less than 40%, the optimal graph is ok, but the optimal values of pseudo-density are all relatively low which should approach to one; (3) when the amount of material is more than 60%, the optimal graph is still nice, but the optimal values of pseudo-density are all relatively high which should near zero. These mean that the object function of structural compliance is somewhat on up side value except the first case. The author deems that it is because 'threshold value' equals to the middle value of standardized 'gradient' whose value is from 0.4 to 0.6. That is why the result of the first case is perfect. By this characteristic, it is reasonable that the 'threshold value' should

have certain relation with 'amount of material' used.

Through the analysis described here, the author proposes the concept of 'modified gradient threshold', which puts 'original threshold value' to multiply the scalar of using material, and divides by 0.4~0.6 to get the value as 'new threshold value'. From the new definition of 'threshold value', we can know that when the amount of using material is between 40% ~60%, it will become the 'original threshold value'. Meanwhile, 'constraint compensation' is still adopted as before.

The general steps of this modified optimality criterion algorithm in iterations can be stated as follows:

1）Gradient of compliance to design variables:

$$\nabla C\left(\overrightarrow{X}\right) = -\left(\overrightarrow{F} \cdot {*}\overrightarrow{U}\left(\overrightarrow{X}\right)\right) \Big/ \overrightarrow{X}$$

2）Standardization of gradient vector

$$\overrightarrow{H}\left(\overrightarrow{X}^{(k)}\right) = \frac{-\nabla C\left(\overrightarrow{X}^{(k)}\right)}{max\left(-\nabla C\left(\overrightarrow{X}^{(k)}\right)\right)}$$

3）'Threshold value' of gradient vector

$$t\left(\overrightarrow{X}^{(k)}\right) = median\left[\overrightarrow{H}\left(\overrightarrow{X}^{(k)}\right)\right] \times \frac{f}{0.4 \sim 0.6}$$

4）Optimal direction

$$\overrightarrow{S}\left(\overrightarrow{X}^{(k)}\right) = sign\left\{\overrightarrow{H}\left(\overrightarrow{X}^{(k)}\right) - t\left(\overrightarrow{X}^{(k)}\right) \cdot \overrightarrow{e}\right\}$$

5）Increment vector of design-variable

$$\Delta\overrightarrow{X}^{(k)} = move\left(\overrightarrow{X}^{(k)}\right) \cdot \overrightarrow{S}\left(\overrightarrow{X}^{(k)}\right)$$

6）Transition vector of design variable

$$\overrightarrow{\overrightarrow{X}}^{(k+1)} = \overrightarrow{X}^{(k)} + \Delta\overrightarrow{X}^{(k)}$$

7）Iterative formula of design variable

$$\overrightarrow{X}^{(k+1)} = min\left\{max\left[\overrightarrow{\overrightarrow{X}}^{(k+1)}, \overrightarrow{X}_{min}^{(k+1)}\right], \overrightarrow{X}_{max}^{(k+1)}\right\}$$

In which operator (.*) and (./) stand for multiplication and division of two vectors that correspond to each element, respectively, the calculated values make up a new vector, for instance: $\overrightarrow{A} \cdot {*}\overrightarrow{B} = \left(a_1 b_1, \cdots, a_n b_n\right)^T$ and $\overrightarrow{A} \Big/ \overrightarrow{B} = \left(a_1 \Big/ b_1, \cdots, a_n \Big/ b_n\right)^T$; operator $max(\bullet)$ stands for fetching maximum value to all elements of a certain vector, its value is a scalar; operator $median[\bullet]$ stands for fetching middle value to all elements of a certain vector, its

value is also a scalar; and operator $sign\{\bullet\}$ stands for sign function, its values are vector; they are all internal function of MATLAB7.1; $\vec{e} = (1, \cdots, 1)^T$; $move(\vec{X})^{(k)}$ stands for move-limit during iterations, its value is a scalar too, here an adaptive move-limit is adopted; $\vec{X}_{min}^{(k+1)}$ and $\vec{X}_{max}^{(k+1)}$ stand for lower and upper bounds of the (k+1)th iterative step respectively. The iterative process and final results show that $\vec{X}_{min}^{(k+1)}$ and $\vec{X}_{max}^{(k+1)}$ may equal to $\vec{X}_{min}$ and $\vec{X}_{max}$ respectively, i.e. the lower and upper bounds of design variables, here they equal to 0.01 and 1 respectively.

Meanwhile, the filtering function proposed by Ole Sigmund is utilized to cancel the phenomena of check-board during iteration [8].

The above algorithm is translated into a modular with MATLAB software and set it in ANSYS computation platform. The flow chart of determining the material optimal layout can outline in figure 3.
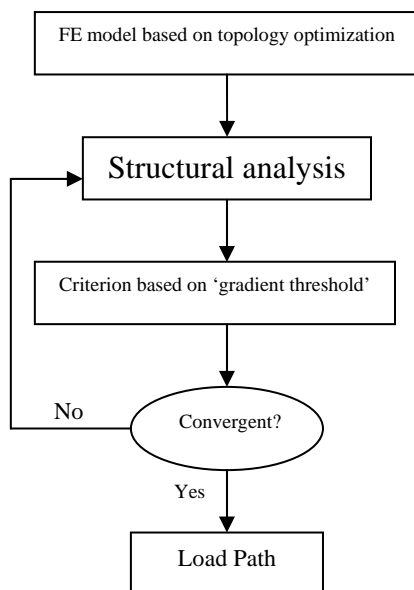
Fig. 3. Flow chart of getting optimal layout

2.2 Sizing Optimization Model of Plate-Rib/Stiffener Structure

The optimization software COMPASS is selected as the platform of computation. Here from the load paths acquired by 'gradient threshold' approach, we can get to know the direction and number of ribs/stiffeners in the plate, which can determine the FEM of plate-rib structure. Next, the thickness of plate and the

sectional area of stiffener are regarded as sizing variables; with FSD method the optimal solution can be gained. The flow chart of sizing optimization can outline in figure 4.
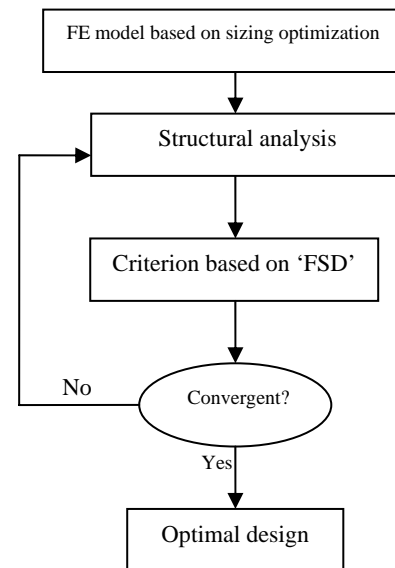
Fig. 4. Flow chart of sizing optimization

2.3 Experiment Principle and Demonstration

According to the optimal design of all sorts of plate-rib structure, the corresponding clamps for the static tests of bending, shear and both loads combined should assort with the components of plate-rib structure, so that all kinds of loads tests are successful to fulfill. Here is the bending load principle, as demonstrated in figure 5.
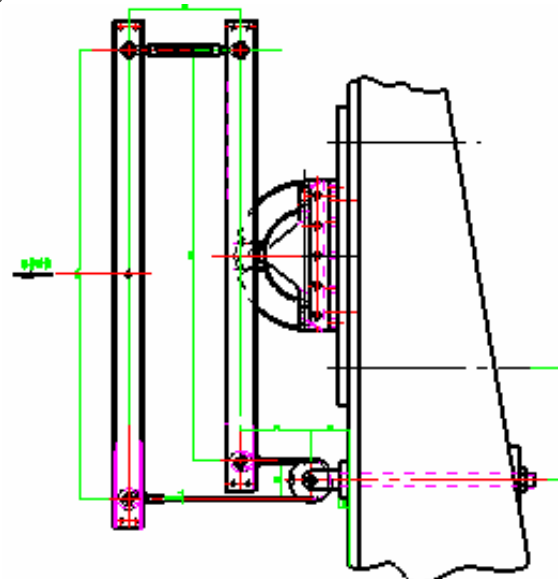
Fig. 5. Principle sketch of bending load test

3 Applications on Plate-Rib Structure

With regard to some designs of bulk heads and a short spar during research, the author simplifies them as dimensions within 400mmX400mm for synthesis and fabrication as well as static test.

Case 1 Bulk Head Passed through Single-Engine for Bending and Shear Load

The initial material distribution and boundary condition of this type of bulk head is demonstrated in a) of figure 6; the optimal load paths (or efficient material distribution) of it as shown in b) of figure 6; the FEM grids of conventional and optimal bulk heads as shown in c) and d) of figure 6, respectively; the design drawings of conventional and optimal bulk heads as shown in e) and f) of figure 6, respectively; the structural responses of these two bulk heads can be seen in table 1.
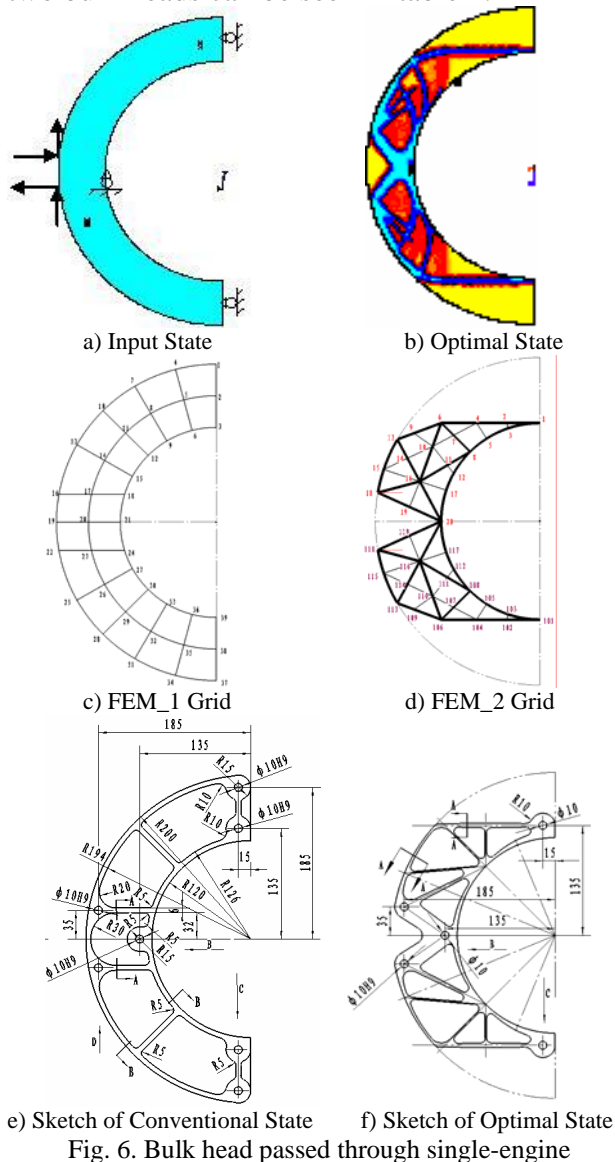
Tab. 1. Structural responses of two kinds of bulk heads

Name	Max-Displacement (mm)	Rod Max Stress (Kg/mm^2)	Plate Max Stress (Kg/mm^2)	FEM Weight (Kg)
Convention	0.5126	27.501	38.325	0.8306
optimality	0.5110	12.809	21.995	0.7912

Case 2 Bulk Head Passed through Double-Engine for Shear Load

The initial material distribution and boundary condition of this type of bulk head is demonstrated in a) of figure 7; the optimal load paths (or efficient material distribution) of it as shown in b) of figure 7; the FEM grids of conventional and optimal bulk heads as shown in c) and d) of figure 7, respectively; the design drawings of conventional and optimal bulk heads as shown in e) and f) of figure 7, respectively; the structural responses of these two bulk heads can be seen in table 2.

a) Input State   b) Optimal State

c) FEM_1 Grid   d) FEM_2 Grid

e) Sketch of Conventional State   f) Sketch of Optimal State
Fig. 6. Bulk head passed through single-engine

a) Input State   b) Optimal State

c) FEM_1 Grid   d) FEM_2 Grid

e) Sketch of Conventional State   f) Sketch of Optimal State
Fig. 7. Bulk head passed through double-engine
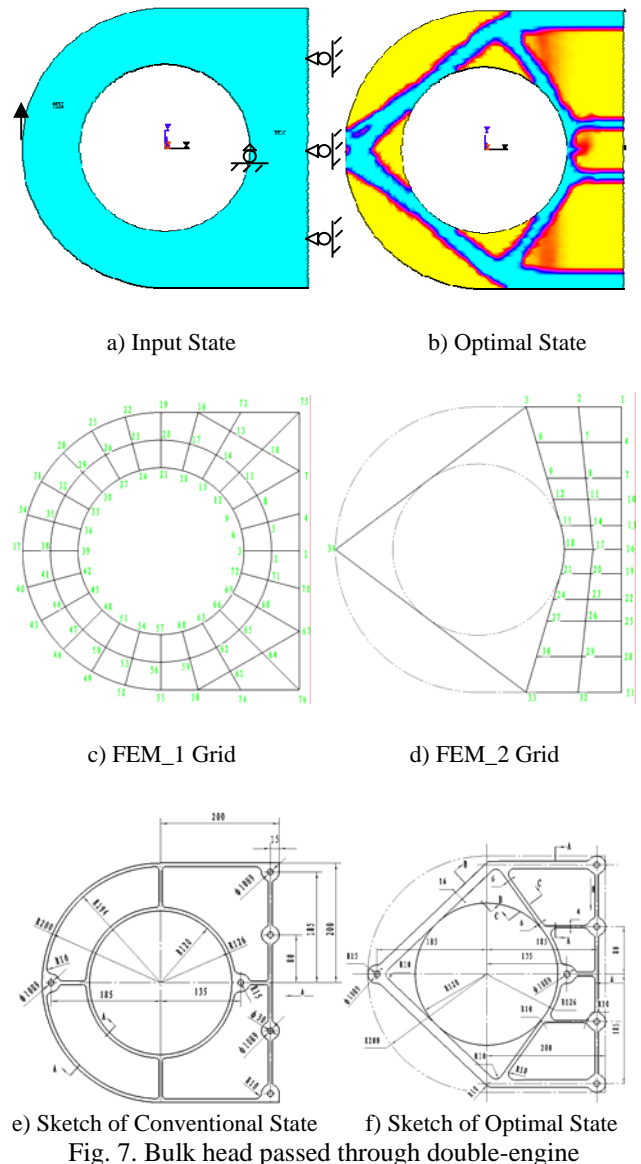
Tab. 2. Structural responses of two kinds of bulk heads

Name	Max-Displacement (mm)	Rod Max Stress (Kg/mm^2)	Plate Max Stress (Kg/mm^2)	FEM Weight (Kg)
Convention	0.3679	3.3078	3.4409	1.6763
optimality	0.3668	2.6015	1.8633	1.3906

Tab. 3. Structural responses of two kinds of bulk heads

Name	Max-Displacement (mm)	Rod Max Stress (Kg/mm^2)	Plate Max Stress (Kg/mm^2)	FEM Weight (Kg)
Convention	0.7733	25.906	25.226	1.60
optimality	0.7711	20.012	22.624	1.33

Case 3 Bulk Head Passed through Double-Engine for Bending and Shear Load

The initial material distribution and boundary condition of this type of bulk head is demonstrated in a) of figure 8; the optimal load paths (or efficient material distribution) of it as shown in b) of figure 8; the FEM grids of conventional and optimal bulk heads as shown in c) and d) of figure 8, respectively; the design drawings of conventional and optimal bulk heads as shown in e) and f) of figure 8, respectively; the structural responses of these two bulk heads can be seen in table 3.

Case 4 Short Spar just for Shear Load

The initial material distribution and boundary condition of this type of short spar is demonstrated in a) of figure 9; the optimal load paths (or efficient material distribution) of it as shown in b) of figure 9; the FEM grids of conventional and optimal short spars as shown in c) and d) of figure 9, respectively; the design drawings of conventional and optimal short spars (plate-rib, truss-like) as shown in e), f) and g) of figure 9, respectively; the structural responses of these three short spars can be seen in table 4.

a) Input State

b) Optimal State

c) FEM_1 Grid   d) FEM_2 Grid

e) Sketch of Conventional State   f) Sketch of Optimal State

Fig. 8. Bulk head passed through double-engine

a) Input State   b) Optimal State

c) FEM_1 Grid   d) FEM_2 Grid

e) Sketch of Conventional State

f) Sketch of Plate-rib State   g) Sketch of Truss-like State
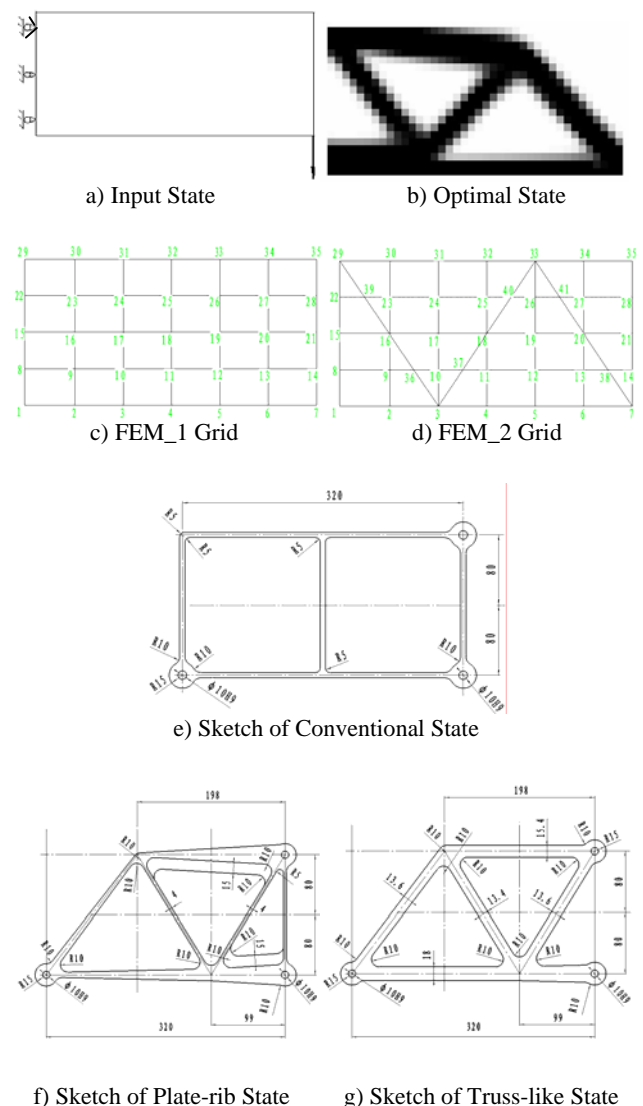
Fig. 9. Short Spar just for shear

Tab. 4. Structural responses of three kinds of short spars

Name	Max-Displacement (mm)	Rod Max Stress (Kg/mm^2)	Plate Max Stress (Kg/mm^2)	FEM Weight (Kg)
Convention	0.8364	9.396	6.732	0.836
Plate-rib	0.8301	5.1	5.1	0.681
Truss-like	0.8345	4.25	/	0.862

4 Experiment Demonstrations

From the final sketches of the nine test parts, they are fabricated and marked component No. 1 till No. 9, orderly, as shown in figure 10. The practical weight of each component can be expressed in table 5.
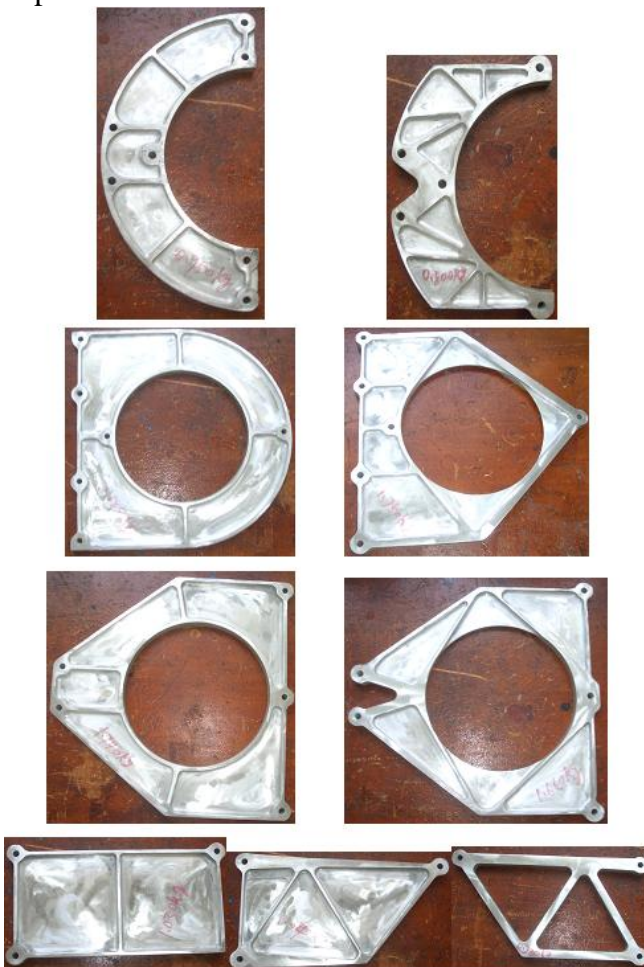
Fig. 10. Photos of nine test parts

Tab. 5. Structural weight of each test part   (unit:Kg)

No.	1	2	3	4	5	6	7	8	9
weight	0.95	0.80	1.89	1.75	1.74	1.66	1.03	1.04	0.98

4.1 Experiment Process and Results

All kinds of test loads process of the nine components and corresponded results can be demonstrated from figure 11 till figure 33, respectively. Here, x-coordinate expresses the equivalent force, its unit is KN; and y-coordinate indicates displacement value of metrical sensor, its unit is mm; the straight line equation stands for the regressive relation of equivalent force and displacement, its slope is the displacement of a unit equivalent force, which is a kind of metric of structural stiffness.
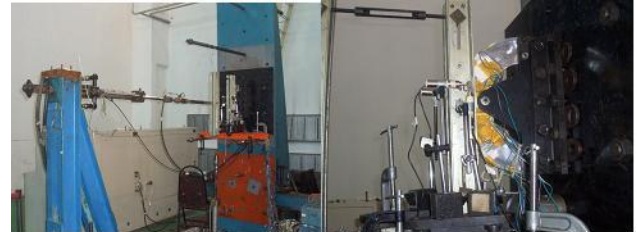
Fig. 11. Bending load process of No. 1 test part
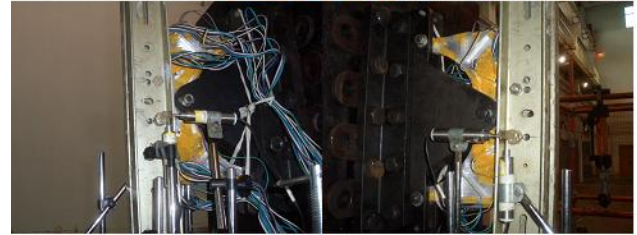
Fig. 12. Bending load process of No. 2 test part

y = 0.0545x + 0.0303

y = 0.0639x + 0.3633
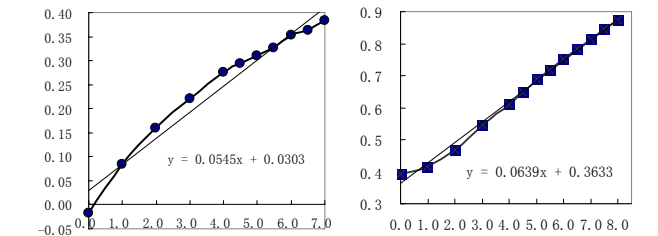
a) Metrical point in left side of No.1   b) Metrical point in left side of No.2

y = −0.0827x + 0.3097

y = −0.0452x + 0.1764
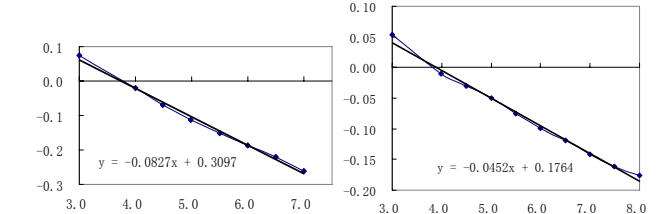
a) Metrical point in right side of No.1 b) Metrical point in right side of No.2

Fig. 13. Horizontal displacement of No.1 and No.2 parts in bending load

y = −0.0114x + 0.785

y = −0.0113x − 0.5491
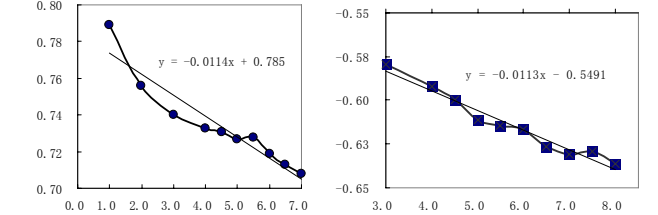
Fig. 14. Vertical displacement of No.1 and No.2 parts in bending load
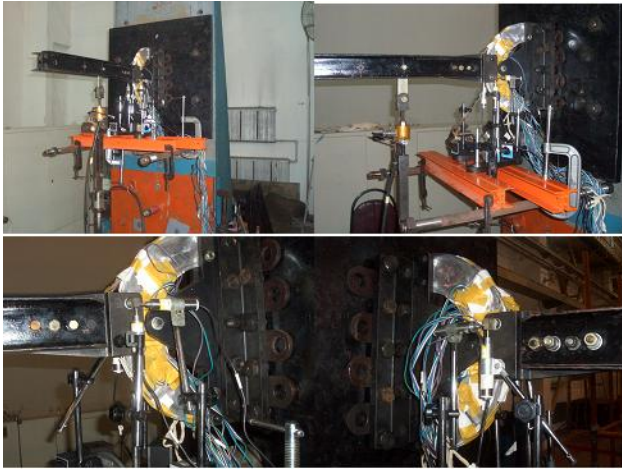
Fig. 15. Combination of bending and shear of No.1 part

Fig. 16. Combination of bending and shear of No.2 part
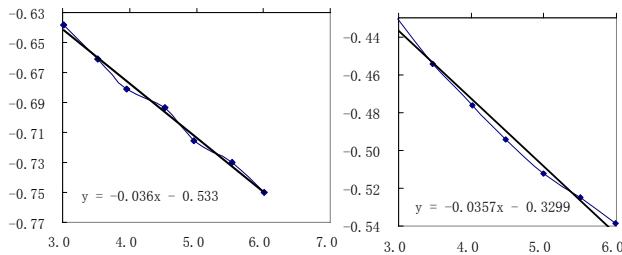
a) Metrical point of No.1 part   b) Metrical point of No.2 part

Fig. 17. Horizontal displacement of No.1 and No.2 parts in bending and shear load

Fig. 18. Shear load process of No. 3 test part

Fig. 19. Shear load process of No. 4 test part
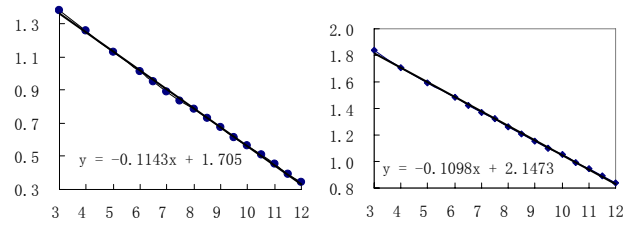
a) Metrical point of No.3 part   b) Metrical point of No.4 part

Fig. 20. Vertical displacement of No.1 and No.2 parts in bending load
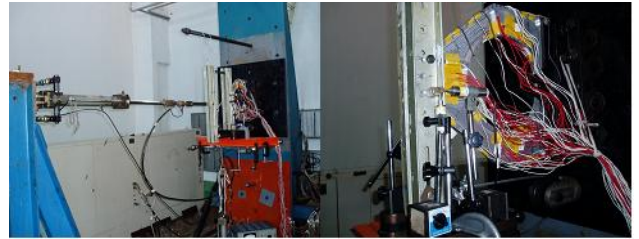
Fig. 21. Bending load process of No.5 test part

Fig. 22. Bending load process of No.6 test part
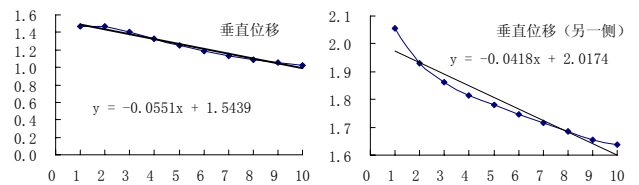
a) Metrical point of No.5 part
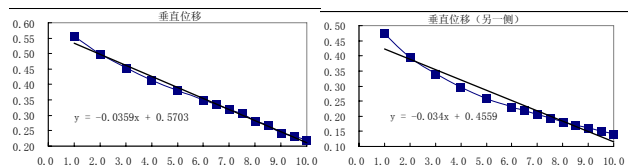
b) Metrical point of No.6 part

Fig. 23. Vertical displacement of No.5 and No.6 parts in bending load
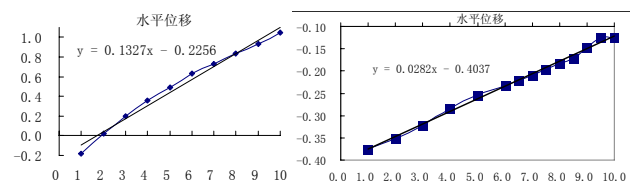
a) Metrical point of No.5 part   b) Metrical point of No.6 part

Fig. 24. Horizontal displacement of No.5 and No.6 parts in bending load

Fig. 25. Combination of bending and shear of No.5 part

Fig. 26. Combination of bending and shear of No.6 part
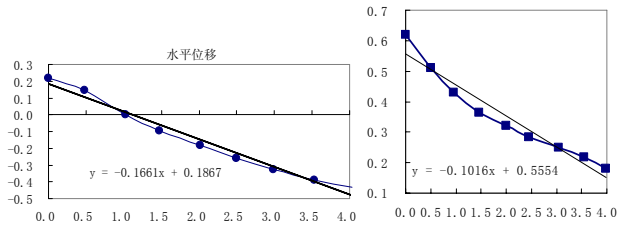
a) Metrical point of No.5 part   b) Metrical point of No.6 part

Fig. 27. Horizontal displacement of No.5 and No.6 parts in bending and shear load
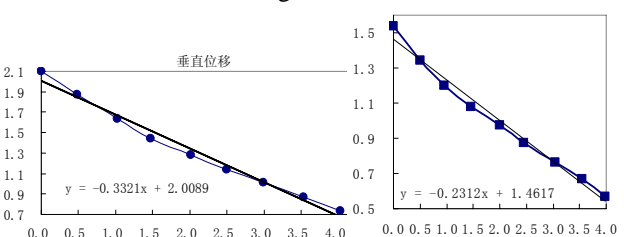
a) Metrical point of No.5 part   b) Metrical point of No.6 part

Fig. 28. Vertical displacement of No.5 and No.6 parts in bending and shear load

Fig. 29. Shear load process of No. 7 test part

Fig. 30. Shear load process of No. 8 test part
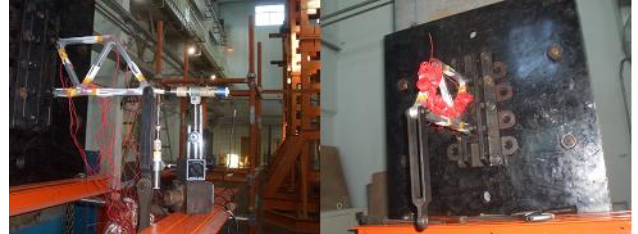
Fig. 31. Shear load process of No. 9 test part
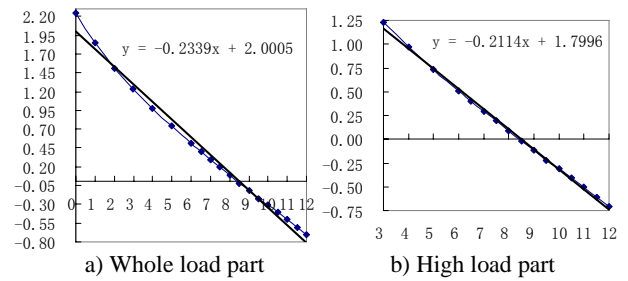
a) Whole load part   b) High load part

Fig. 32. Vertical displacement of No.7 parts in shear load
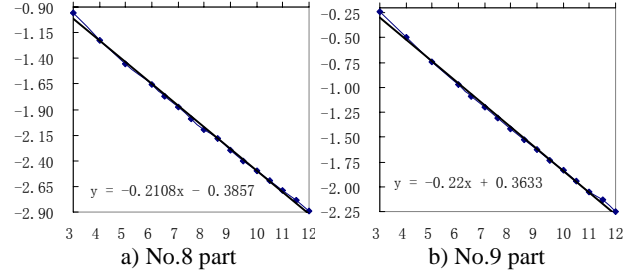
a) No.8 part   b) No.9 part

Fig. 33. Vertical displacement of No.8 and No.9 parts in shear load

4.2 Analysis of Experiment Results

From the experiment curves of part No.1~part No.9 in the above section and adding the consideration of error fabrication to the effect of each component's weight, as shown in table 5, the stiffness difference metric (displacement under a unit load) of every component can be calculated, and the improved percentage (IP) of them is also calculated, as expressed in table 6.

Tab. 6 Component displacement under a unit load

Load	Bending		Shear		Bending&Shear	
Dis	Hor	Ver	Hor	Ver	Hor	Ver
No.1	.0815	.0135	/	/	/	.0428
No.2	.0546	.0113	/	/	/	.0357
IP	33%	19.5%	/	/	/	19.9%
No.3	/	/	.1231	/	/	/
No.4	/	/	.1098	/	/	/
IP	/	/	12.1%	/	/	/

No.5	.1327	.0485	/	/	.1661	.3321
No.6	.0282	.0349	/	/	.1016	.2312
IP	21.3%	39.0%	/	/	38.8%	30.4%
No.7	/	/	/	.2222	/	/
No.8	/	/	/	.2237	/	/
No.9	/	/	/	0.22	/	/

Analysis to the experiment data in table 6, we can find that the structural stiffness of optimal component can be increased from 20% to 30% compared with that of conventional component corresponded.

5 Discussions and Analysis

From the compared values of the corresponded two types plate-stiffener, as outlined in table1~table4, some useful data can be obtained, as shown in table 7.

Tab. 7. Variation of structure response (equal stiffness)

Name		Fig. 6	Fig. 7	Fig. 8	Fig. 9
Max stress decrease	Rod	53.4%	21.3%	22.6%	45.7%
	Plate	42.6%	45.8%	10.3%	24.2%
FEM weight decrease		5.0%	20.5%	20.3%	22.8%

From the values in table 7, we can find the fact: on the condition of equal stiffness, whether the max stress, or the structure weight of component, the parts with most efficient load paths are much better than those of conventional plate-rib. For example, the structure weight savings are among 5%~20%; in the same way, the max stress decrease is in the range from 10% to 50%.

Through analysis in more details, the author deems that there are three reasons to explain the above. One is that the proposed method put the material on the load paths through topology optimization; this makes the structure more rational and the material more efficient. Nevertheless, it is hard to put the material on the very load paths by way of conventional approach, due to the load paths sometimes not visually obvious. Next, the proposed method can cut off the material which is inefficient, but the conventional approach generally can not. Last, the ribs/stiffeners and plate combine with each other to bear the loads; this improves the structure efficiency remarkably. Usually, the stress on stiffeners of conventional plate is much lower because the stiffeners are not exactly on the load paths.

6 Summaries

With regard to the numerical optimization design and experiment demonstration of air craft plate-rib/stiffener structure, four concluding remarks can be drawn from the work being done in this article. They are in below:

(1) The authors set forth an idea that topology optimization was used to determine the load paths of these two-dimension components which belong to typical structure of aircraft. Numerical examples and experiment demonstration showed that the approach is effective and operational, which generally differs from traditional design method based on experience and intuition of the designer.

(2) Comparing with the traditional design method, the light-weight design approach based on the combination of topology and sizing optimization can remarkably increase the structural responses of components which are dealt with.

(3) The posed approach is also suitable for designing other 2-D parts of aircraft.

(4) From the work being done, the design process is lucid and suitable for designing plate-rib/stiffener structures from conceptual design to preliminary and even to detail design.

References

[1] Thomas C. Corke, Design of Aircraft, Prentice Hall, 2003.

[2] Deng YC, Zhang WH, Zhu JH, Zhang YN. Structural design of wing thin-walled box. Mechanics in Engineering, 2004,26(6):20~22(in Chinese) .

[3] Lars Krog, Application of topology, sizing and shape optimization methods to optimal design of aircraft components, Alastair Tucker and Gerrit Rollema Airbus UK Ltd, Advanced Numerical Simulations Department, Bristol, BS 99 7AR.

[4] Deng YC, Zhang WH, Wan M, Zhang YN. Structural layout for aircraft movable wing. Mechanics in Engineering, 2004, 26(5):14~17(in Chinese).

[5] Deng YC, Chen H, Ma ML, Zhang YN. Studies of Aircraft Frame Design based on Topology Optimization. Strength & Environment, 1006-3919(2005)02-0039-07(in Chinese).

[6] Deng YC, Li XJ, Zhu JH, Chen H. An Application of Aircraft Strengthen Frame Design Based on Gradient Variable-Threshold Topology Optimization. Mechanics in Engineering, 2005, 27(4):26~31(in Chinese).

[7] Deng, YC. An Application of Aircraft Structural Part Conceptual Design Based on Topology Optimization Method, The Fourth China-Japan-Korea Joint Symposium on Optimization of Structural and Mechanical Systems, Kunming, Nov.6-9, 2006, China.

[8] M. P. Bendsee and O. Sigmund., Topology optimization-Theory, method and applications. Springer Verlag Berlin, Heidelberg, New York, 2003.

Acknowledgement

Copyright Statement